Development 129, 2109-2119 (2002)
Printed in Great Britain © The Company of Biologists Limited 2002
DEV2803

Heparan sulphate proteoglycans and spinal neurulation in the mouse embryo

George W. Yip[1,*], Patrizia Ferretti[1] and Andrew J. Copp[2,†]

[1]Developmental Biology Unit, Institute of Child Health, University College London, London, UK
[2]Neural Development Unit, Institute of Child Health, University College London, London, UK
*Present address: Department of Anatomy, National University of Singapore, Singapore
†Author for correspondence (e-mail: a.copp@ich.ucl.ac.uk)

Accepted 12 February 2002

SUMMARY

Heparan sulphate proteoglycans have been implicated in the binding and presentation of several growth factors to their receptors, thereby regulating cellular growth and differentiation. To investigate the role of heparan sulphate proteoglycans in mouse spinal neurulation, we administered chlorate, a competitive inhibitor of glycosaminoglycan sulphation, to cultured E8.5 embryos. Treated embryos exhibit accelerated posterior neuropore closure, accompanied by suppression of neuroepithelial bending at the median hinge point and accentuated bending at the paired dorsolateral hinge points of the posterior neuropore. These effects appear specific, as they can be prevented by addition of heparan sulphate to the culture medium, whereas heparitinase-treated heparan sulphate and chondroitin sulphate are ineffective. Both N- and O-sulphate groups appear to be necessary for the action of heparan sulphate. In situ hybridisation analysis demonstrates a normal distribution of sonic hedgehog mRNA in chlorate-treated embryos. By contrast, patched 1 transcripts are abnormally abundant in the notochord, and diminished in the overlying neuroepithelium, suggesting that sonic hedgehog signalling from the notochord may be perturbed by inhibition of heparan sulphation. Together, these results demonstrate a regulatory role for heparan sulphate in mouse spinal neurulation.

Key words: Chlorate, Glycosaminoglycans, Heparan sulphate, Neural tube defects, Patched, Proteoglycans, Sonic hedgehog, Extracellular matrix

INTRODUCTION

Neurulation is a fundamental morphogenetic event that culminates in the elevation, apposition and fusion of the neural folds in the dorsal midline (Copp et al., 1990; Smith and Schoenwolf, 1997). Failure of neural tube closure leads to the clinically important birth defects spina bifida and anencephaly (Copp and Bernfield, 1994). Although the molecular mechanisms that control neural tube closure are poorly understood, a role for extracellular signalling mechanisms is emerging. For example, mice that lack the function of fibroblast growth factor (FGF) receptor 1, which transduces the signalling of several FGFs, exhibit defective closure of the caudal neural folds (Deng et al., 1997). A similar defect arises in mice homozygous for the *curly tail* (*ct*) mutation, in which reduced expression of the *Wnt5a* gene has been identified (Gofflot et al., 1998). Moreover, recent studies demonstrate a critical role for sonic hedgehog (Shh) signalling in the regulation of neural plate bending in the spinal region of the mouse embryo (Ybot-Gonzalez et al., 2002). Hence, three distinct signalling pathways have been implicated in mouse spinal neurulation. A common feature of these signalling pathways is the role played by heparan sulphate proteoglycans (HSPGs) in the presentation of ligands to responding cells. The present study examines the role of HSPGs in mouse spinal neurulation.

Heparan sulphate is a glycosaminoglycan (GAG) of repeating disaccharide subunits, comprising glucosamine and glucuronic/iduronic acid, covalently linked to a core protein backbone (Bernfield et al., 1999). A family of HSPGs exists, some of which are localised to the cell surface through a transmembrane core protein (syndecans) or by a glycosylphosphatidylinositol linkage (glypicans), while others form part of the extracellular matrix (perlecan and agrin). HSPGs bind to and regulate the activity of many important signalling molecules. For example, analysis of the *Drosophila tout-velu* mutant and the *Ext1*-deficient mouse, both of which lack heparan sulphate co-polymerase, shows that HSPGs are essential for the function of several members of the hedgehog family of signalling proteins (Bellaiche et al., 1998; Lin et al., 2000; The et al., 1999). Similarly, examination of the *Drosophila sugarless* and *sulfateless* mutants provides evidence for a role of HSPGs in fibroblast growth factor (FGF) and Wnt signalling (Häcker et al., 1997; Lin et al., 1999). Furthermore, tissue-specific developmental defects are seen after modification of the number and position of the sulphate groups on heparan sulphate. For example, mice homozygous for the *Hs2st* gene trap mutation are unable to add 2-O sulphate groups to heparan sulphate and exhibit renal, eye and skeletal defects (Bullock et al., 1998), while targeted disruption of the *Ndst1* gene, which encodes N-deacetylase N-sulphotransferase 1, leads to pulmonary hypoplasia, atelectasis and respiratory distress syndrome (Ringvall et al., 2000).

HSPGs are found in the basement membrane of the neuroepithelium of the closing neural tube, as well as in the adjacent tissues of the posterior neuropore region (Copp and Bernfield, 1988; O'Shea, 1987). Moreover, degradation of heparan sulphate by heparitinase disrupts cranial neurulation in cultured rat embryos, leading to the development of exencephaly (Tuckett and Morriss-Kay, 1989). The purpose of the present study was to determine whether HSPGs, and specifically the sulphation pattern of heparan sulphate, could also regulate spinal neurulation. We cultured E8.5 mouse embryos in the presence of an inhibitor of sulphation, chlorate, to examine the importance of the sulphate group in HSPG function. The sulphate donor for GAG sulphation is 3′-phosphoadenosine 5′-phosphosulphate (PAPS), which is synthesised by PAPS synthetase. Chlorate acts as a sulphate analogue and competes with sulphate in PAPS synthesis, resulting in inhibition of GAG sulphation (Conrad, 1998; Greve et al., 1988). We find that chlorate acts to hasten the closure of the spinal neural tube, and we present evidence suggesting that this effect may be mediated, in part, via inhibition of Shh signalling.

MATERIALS AND METHODS

Culture of intact embryos

Random-bred CD1 mice were mated overnight and the day of finding a copulation plug was designated embryonic day (E) 0.5. Embryos at E8.5 were explanted into Dulbecco's modified Eagle's medium (DMEM) containing 10% foetal calf serum and cultured in undiluted rat serum, in a roller incubator maintained at 38°C (Copp et al., 2000). Cultures were stabilised over a 3 hour period, then chlorate, β-D-xyloside (p-nitrophenyl-β-D-galactopyranoside), sulphate, bovine kidney heparan sulphate, shark cartilage chondroitin-4-sulphate or chondroitin-6-sulphate (all from Sigma), or chemically modified bovine kidney heparan sulphate (Seikagaku) were added in various combinations and culture was continued for 14 hours. Heparan sulphate was degraded by incubation with 0.1 U/ml heparitinase (Seikagaku) at 37°C overnight, and the enzyme was then heat inactivated.

After culture, embryos were selected for further analysis only if they exhibited vigorous blood flow in the yolk sac circulation, and if the heart beat was regular and above 100 per minute. They were dissected from the yolk sac and amnion, inspected for closure of the cranial and spinal neural tube, then scored using the Morphological Scoring System of Brown and Fabro (Brown and Fabro, 1981). Crown-rump length, head length and posterior neuropore length (the distance between the rostral end of the posterior neuropore and the tip of the tail bud) were measured using an eyepiece graticule attached to a Zeiss SV6 stereomicroscope. Some embryos were sonicated and used to determine total protein content using the BCA Protein Assay Kit (Pierce and Warriner), whereas others were fixed in 4% paraformaldehyde in phosphate-buffered saline (PBS) before embedding in paraffin wax and sectioning at 6 μm, transversely through the posterior neuropore region. Sections were stained with Haematoxylin and Eosin or used for immunolocalisation of chondroitin sulphate and heparan sulphate. Other embryos were processed for whole-mount mRNA in situ hybridisation for *Shh* and patched 1 (*Ptch*).

Immunohistochemistry

Mouse monoclonal antibodies 10E4 (Seikagaku) and CS-56 (Sigma) were used to detect heparan sulphate and chondroitin sulphate respectively (Avnur and Geiger, 1984; David et al., 1992). A monoclonal mouse IgM antibody (DAKO) raised against *Aspergillus niger* glucose oxidase (an enzyme neither present nor inducible in mammalian tissues) was used as a negative control. Rehydrated tissue sections were incubated with 3% hydrogen peroxide and the blocking solutions from the HistoMouse-SP kit (Zymed) to reduce nonspecific background staining, then incubated with 10 μg/ml primary antibody for an hour at room temperature. The signal was amplified using a biotinylated anti-mouse secondary antibody and a streptavidin-horseradish peroxidase conjugate and detected using 3,3′-diaminobenzidine tetrahydrochloride.

Labelling and analysis of GAGs

GAGs were labelled using carrier-free [^{35}S]sulphate and analysed by anion exchange chromatography (Solursh and Morriss, 1977; Copp and Bernfield, 1988). Embryos were stabilised in culture for 3 hours, then carrier-free [^{35}S]sulphate (Amersham Pharmacia) was added to the culture medium to a final concentration of 100 μCi/ml (final concentration of sulphate: 0.75 μM) and culture was continued for a further 5 hours. After removal of yolk sac and amnion, embryos were washed using ice-cold DMEM and PBS in order to remove unincorporated label. Embryos were stored in TE (50 mM Tris, pH 7.5; 2 mM EDTA) at –70°C.

Labelled GAGs were extracted by sonicating embryos in TE on ice. An aliquot was removed for scintillation counting and protein quantification, then 50 μg each of carrier hyaluronan and chondroitin-6-sulphate (Sigma) were added and GAGs were precipitated overnight at –20°C using three volumes of 1.3% potassium acetate in 95% ethanol. GAGs were pelleted by centrifugation at 14,000 ***g*** for 15 minutes, then re-suspended in de-ionised water. Pronase (Protease XIV, Sigma) was added (2 mg) and samples were incubated at 55°C overnight to degrade proteins. The enzyme was heat-inactivated, the GAGs were re-precipitated using potassium acetate and ethanol, and the pellet was dissolved in de-ionised water.

Labelled GAGs were separated by anion exchange chromatography on DEAE cellulose (DE52; Whatman) using a linearly increasing elution gradient of sodium chloride solution (up to 0.7 M), at a flow rate of 15 ml/hour. Total elution volume was 25 ml and fractions were collected at 2-minute intervals. Radioactivity in each fraction was measured using a Wallac 1410 liquid scintillation counter. Recovery from the anion exchange column was 99.3±0.4%. The efficiency of scintillation counting was 87.1%.

In situ hybridisation

Whole-mount in situ hybridisation using digoxigenin-labelled riboprobes was performed as described (Tautz and Pfeiffle, 1989), using plasmids for *Shh* (Echelard et al., 1993) and *Ptch* (Goodrich et al., 1996). Briefly, embryos fixed in 4% paraformaldehyde and stored in 100% methanol were rehydrated, incubated in 6% hydrogen peroxide for 1 hour, and then digested with Proteinase K (10 μg/ml) for 2 minutes. The embryos were re-fixed in 0.2% glutaraldehyde and 4% paraformaldehyde, and hybridised overnight at 70°C. After high stringency washes, the riboprobes were localised using a sheep anti-digoxigenin antibody and detected by incubation in nitroblue tetrazolium/5-bromo-4-chloro-3-indolyl phosphate. Transverse paraffin wax-embedded sections (10 μm) were prepared through the posterior neuropore region.

Statistical analysis

Embryonic parameters were compared between treatment groups by Student's *t*-test or one-way analysis of variance, with subsequent pairwise comparisons against the PBS-treated control group by Dunnett's test. Statistical significance level was $P<0.05$.

RESULTS

Titration of chlorate concentration

Chlorate concentrations of up to 30 mM have been used in both cell and organ cultures to inhibit sulphation, with no significant effect on GAG or protein synthesis or on cell viability (Conrad,

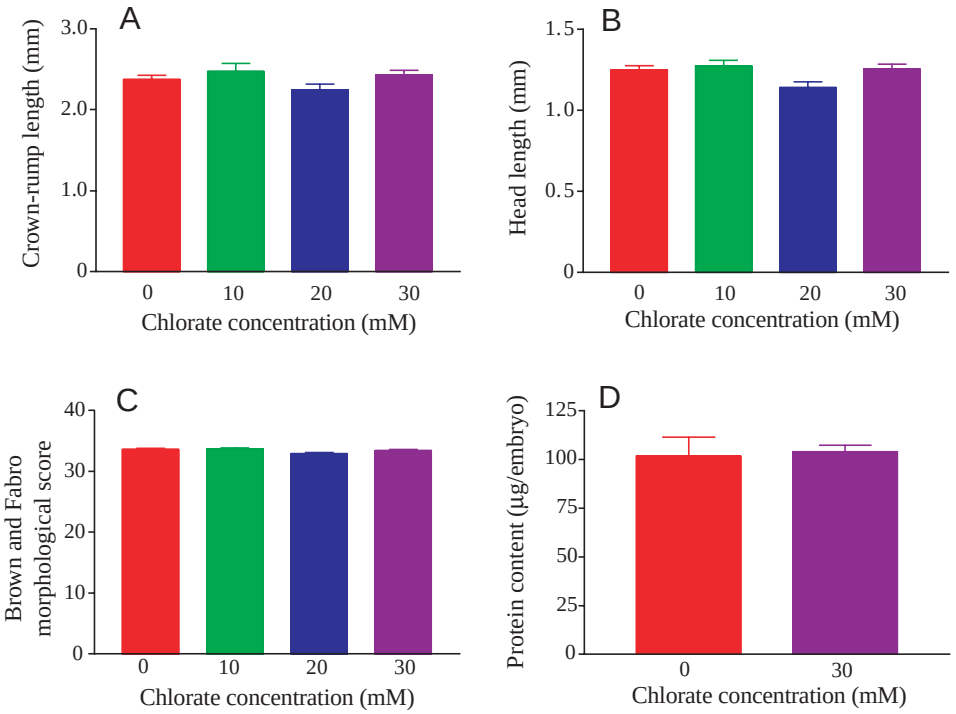

Fig. 1. Effect of chlorate on embryonic growth parameters. (A) Crown-rump length, (B) head length and (C) Brown and Fabro morphological score of E9.5 embryos following culture for 14 hours in the presence of 0, 10, 20 and 30 mM chlorate. Statistical comparison using one-way ANOVA shows no significant effect of chlorate concentration on any of the growth parameters (P=0.307, 0.178, 0.308 in A,B,C, respectively). (D) Total embryonic protein content does not differ between cultures containing 0 and 30 mM chlorate (Student's t-test; p=0.854). Values represent mean±s.e.m. of at least 9 embryos in each group in A-C, and at least five embryos per group in D.

1998; Davies et al., 1995; Greve et al., 1988; Miao et al., 1996). Initially, therefore, we performed a titration series in cultures of whole mouse embryos in order to identify a chlorate concentration that might affect spinal neural tube closure without generalised toxic effects on embryonic growth and development. Embryos were explanted from the uterus between the 10- and 14-somite stages, stabilised in culture for 3 hours, then cultured in the presence of different concentrations of chlorate for 14 hours.

All embryos exposed to chlorate concentrations of 30 mM or less had a vigorous yolk sac circulation and regular heart beat. Moreover, comparison of crown-rump length, head length, Brown and Fabro morphological score and protein content showed no statistically significant differences between embryos treated with chlorate and those in the control group, cultured in the absence of chlorate (Fig. 1). All embryos had between 19 and 23 pairs of somites with no significant difference in somite number between treatment groups (Fig. 2A). No obvious difference in gross morphology was found between the two groups, apart from the posterior neuropore length, which differed significantly as described in the following sections.

Inhibition of GAG sulphation results in accelerated posterior neuropore closure

The posterior neuropore is a region of unclosed neural folds at the caudal end of the E8.5-E10 embryo (Van Straaten et al., 1992). To determine whether inhibition of GAG sulphation has an effect on spinal neurulation, posterior neuropore length was compared among embryos cultured in the presence of different chlorate concentrations (Fig. 2B). Those exposed to 30 mM chlorate showed a statistically significant reduction of 34.2% in posterior neuropore length compared with embryos that

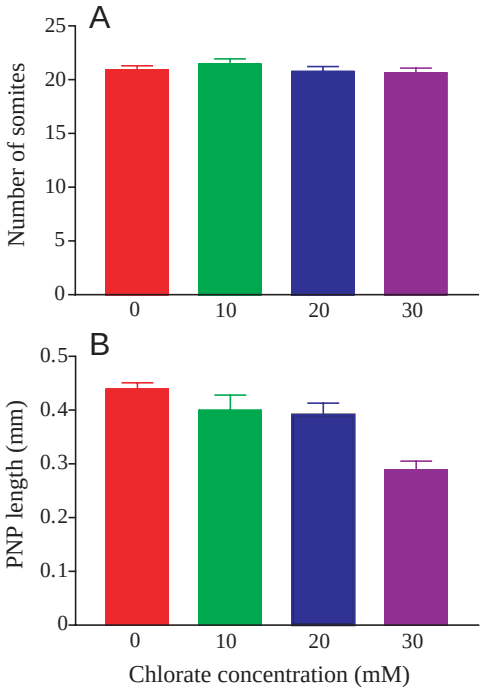

Fig. 2. Effect of chlorate on developmental progression and closure of the spinal neural tube. E9.5 embryos following culture for 14 hours in the presence of 0, 10, 20 or 30 mM chlorate. Comparison of somite number (A) and posterior neuropore length (B) between the four groups using one-way ANOVA shows no significant effect of chlorate concentration on somite number (P=0.641) but a significant effect on neuropore length (P<0.0001) which is significantly smaller in embryos treated with 30 mM chlorate than in the 0 mM group (Dunnett's test; P<0.01). Treatment with 10 mM and 20 mM chlorate did not significantly reduce the posterior neuropore length compared with the 0 mM group (P>0.05 in each case). Values represent mean±s.e.m. of at least nine embryos in each group. PNP, posterior neuropore.

were not exposed to chlorate, whereas no statistically significant difference in posterior neuropore length occurred in embryos cultured in the presence of up to 20 mM chlorate. Hence, closure of the posterior neuropore appears to be accelerated by chlorate treatment, an effect that is specific for spinal neurulation and not secondary to either developmental retardation (as somite number is not affected, Fig. 2A) or growth retardation (as all growth parameters are normal, Fig. 1). All subsequent experiments were carried out at a chlorate concentration of 30 mM.

In contrast to chlorate, there was no significant effect of 1 mM β-D-xyloside on posterior neuropore closure (not shown), whereas cranial neurulation was frequently disturbed, as described previously (Morriss-Kay and Crutch, 1982). Moreover, caudal somitogenesis was disturbed in β-D-xyloside-treated embryos, but not in chlorate-treated embryos. Hence, chlorate and β-D-xyloside have differing effects on neurulation in the spinal and cranial regions.

To confirm that the effect of chlorate is due to competitive inhibition of GAG sulphation, embryos were cultured in the presence of PBS, chlorate, or chlorate plus sulphate. Exogenous sulphate in the culture medium is predicted to compete out the effect of chlorate in inhibiting GAG sulphation. As in the dose-response experiment (Fig. 2B), we found that 30 mM chlorate leads to a reproducible shortening of the posterior neuropore (Fig. 3A). Moreover, exogenous sulphate (10 mM) was able to block the effect of chlorate in inducing premature neuropore closure ($P<0.01$). There was no difference in posterior neuropore length between embryos cultured in the presence of chlorate plus sulphate and those exposed to PBS ($P>0.05$). Hence, acceleration of posterior neuropore closure by chlorate is due to competitive inhibition of GAG sulphation.

Specific requirement for heparan sulphate in posterior neuropore closure

Heparan sulphate and chondroitin sulphate are the principal sulphated GAGs synthesised by the mouse embryo during neurulation (Copp and Bernfield, 1988; Solursh and Morriss, 1977). To assess their relative requirements for posterior neuropore closure, embryos were cultured in the presence of chlorate together with either exogenous heparan sulphate or chondroitin sulphate. Heparan sulphate effectively blocked the action of chlorate on posterior neuropore closure (Fig. 3B), so that posterior neuropore length did not differ between embryos cultured in the presence of both chlorate and heparan sulphate, and those exposed to PBS ($P>0.05$). However, heparan sulphate that had been degraded by overnight treatment with heparitinase before addition to cultures was unable to block the effect of chlorate in accelerating posterior neuropore closure (Fig. 3C). Exogenous chondroitin-4-sulphate (not shown) and chondroitin-6-sulphate (Fig. 3D) also failed to prevent the chlorate-induced effect on posterior neuropore closure. These findings suggest that an intact heparan sulphate chain is required to counteract the effect of chlorate on spinal neurulation.

Effect of chlorate on GAG sulphation

We studied the effect of chlorate on GAG sulphation by culturing embryos in the presence of [^{35}S]sulphate followed by extraction of ^{35}S-labelled GAGs and analysis by anion exchange chromatography. Because the molar concentration of sulphate in these cultures was 1.3×10^4 times lower than in the blocking experiments (Fig. 3A), the addition of [^{35}S]sulphate was not expected to block the effect of chlorate.

Embryos cultured in the absence of chlorate gave an elution profile (red line, Fig. 4A) in which heparan sulphate eluted at a sodium chloride concentration of 0.33±0.01 M (mean±s.e.m.) and was sensitive to heparitinase digestion (not shown), while chondroitin sulphate eluted at a sodium chloride concentration

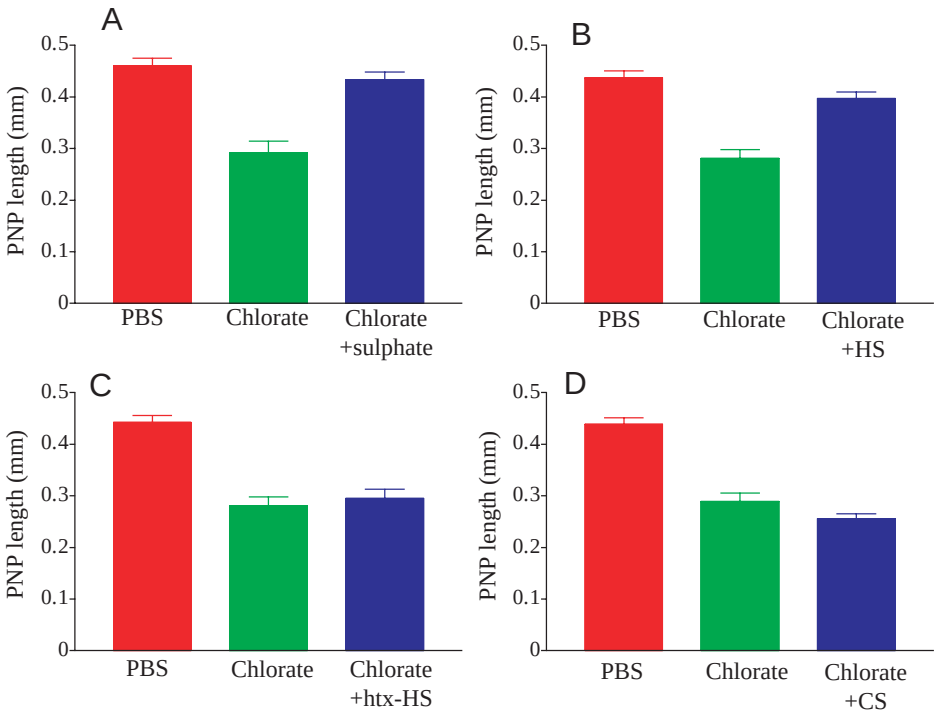

Fig. 3. Specific requirement for heparan sulphate in spinal neurulation. Embryos were cultured in the presence of PBS, 30 mM chlorate alone or 30 mM chlorate plus (A) 10 mM sulphate, (B) 100 ng/ml heparan sulphate, (C) 100 ng/ml heparan sulphate pre-treated with heparitinase or (D) 100 ng/ml chondroitin-6-sulphate. Posterior neuropore length varies significantly between treatment groups (one-way ANOVA; $P<0.0001$) in all panels with a significantly shorter posterior neuropore length in the chlorate alone group compared with the PBS-treated group in each case (Dunnett's test: $P<0.01$). Embryos treated with chlorate plus exogenous sulphate (A) or heparan sulphate (B) do not differ in posterior neuropore length significantly from PBS-treated embryos ($P>0.05$), while embryos treated with chlorate plus heparitinase-treated heparan sulphate (C) or chondroitin-6-sulphate (D) do not differ from embryos treated with chlorate alone ($P>0.05$). Values represent mean±s.e.m. of at least 12 embryos per group in A-C and at least nine embryos per group in D. CS, chondroitin-6-sulphate; HS, heparan sulphate; htx-HS, heparitinase-treated heparan sulphate.

of 0.43±0.01 M and was sensitive to digestion by chondroitinase ABC. By contrast, in cultures of chlorate-treated embryos (green line, Fig. 4A), sulphation of chondroitin sulphate was completely abolished, while the degree of sulphation of heparan sulphate was reduced by 46.0%, giving rise to Peak HS′. This incomplete abolition of heparan sulphation probably results from chlorate (30 mM) inhibiting O-sulphation more effectively than N-sulphation (Safaiyan et al., 1999).

Importantly, addition of exogenous heparan sulphate (100 ng/ml) to the culture medium did not block the effect of chlorate in inhibiting GAG sulphation (blue line, Fig. 4A). This finding demonstrates that the action of exogenous heparan sulphate in abrogating the chlorate effect on neuropore closure (Fig. 3B) is not via a diminution of the inhibitory action of chlorate on sulphation of endogenously synthesised heparan sulphate. Rather, exogenous heparan sulphate seems to have a more direct effect, making good the deficiency of sulphated endogenous heparan sulphate in the embryonic tissues.

We treated samples of material from Peak HS′ with chondroitinase, heparitinase or PBS before analysis using anion exchange chromatography (Fig. 4B). Chondroitinase had no effect on Peak HS′, whereas heparitinase reduced its height to give Peak HS″, thus confirming that Peak HS′ consists of under-sulphated heparan sulphate.

Requirement for both N- and O-sulphate groups in heparan sulphate

Heparan sulphate contains both N- and O-linked sulphate groups. To determine which is needed for regulating spinal neurulation, embryos were cultured in the presence of chlorate plus either de-N- or de-O-sulphated heparan sulphate. Neither heparan sulphate species was able to prevent the neuropore closure effect of chlorate (Fig. 5), suggesting that both N- and O-sulphate groups are needed for heparan sulphate to regulate spinal neurulation.

Effect of chlorate on neuroepithelial bending

Next, we studied the morphology of the posterior neuropore in embryos exposed to chlorate in culture (Fig. 6). Gross observation of chlorate-treated embryos revealed that, in addition to their reduced neuropore length, a marked convexity is invariably present in the neural plate of the neuropore region (Fig. 6B). This contrasts with the normal posterior neuropore morphology observed in PBS-treated embryos (Fig. 6A) and in embryos treated with chlorate plus exogenous heparan sulphate (Fig. 6C).

Transverse histological sections (Fig. 6D) confirm that the E9.5 posterior neuropore exhibits a median hinge point overlying the notochord, together with paired dorsolateral hinge points on the neural folds (Fig. 6E). These hinge points help to elevate the neural folds and bring the fold apices into apposition in the dorsal midline. The non-bending regions of the neural plate lying between the median and dorsolateral

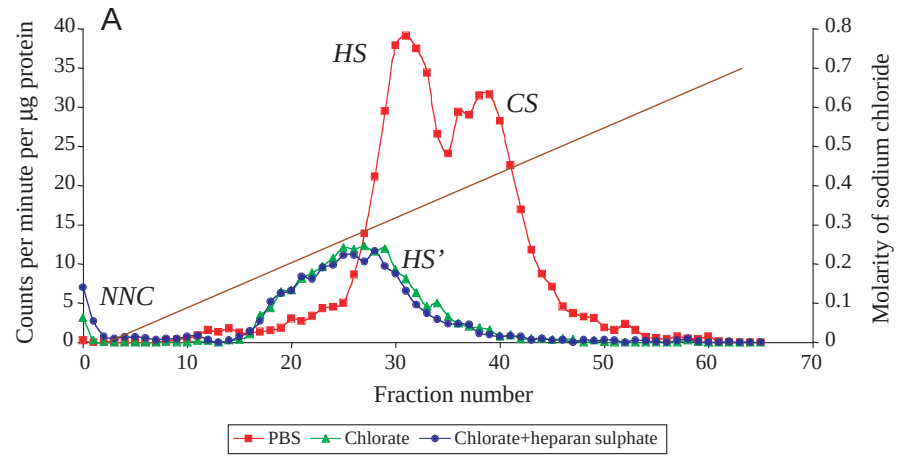

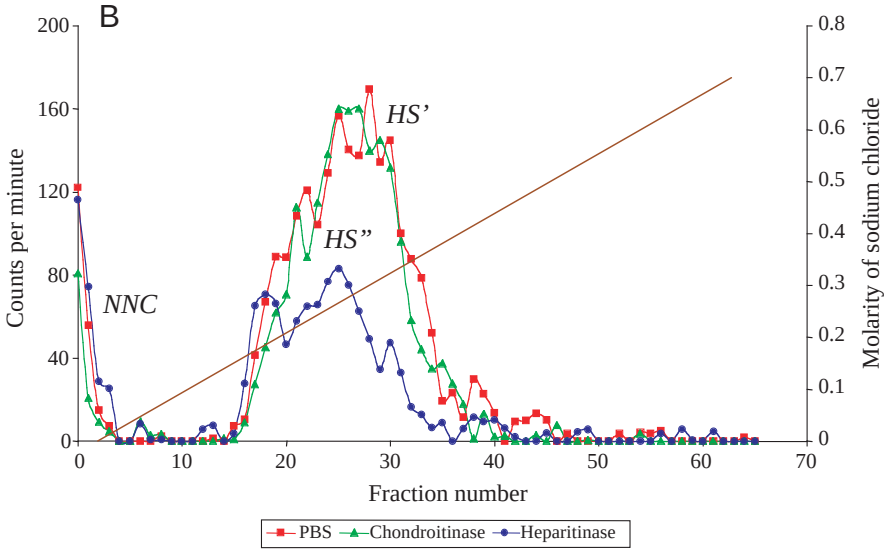

Fig. 4. Chlorate inhibits sulphation of GAGs in cultured mouse embryos. (A) [^{35}S]sulphate-labelled GAGs from PBS-treated embryos were separated by anion exchange chromatography, yielding two peaks (red line), representing heparan sulphate (HS) and chondroitin sulphate (CS). Culture of embryos in chlorate (green line) abolishes sulphation of chondroitin sulphate and dramatically reduces the sulphation of heparan sulphate, resulting in the formation of Peak HS′. There is no effect on the elution profile when exogenous heparan sulphate (100 ng/ml) is added to the chlorate-treated embryos (blue line). (B) The single ^{35}S-labelled GAG peak (HS′) from chlorate-treated embryos (red line) is unaffected by pre-treatment with chondroitinase (green line), whereas it is significantly reduced in height by heparitinase treatment, giving rise to Peak HS″ (blue line). Note the expanded *y*-axis used for plotting the level of radioactivity in B compared with A. Brown line represents elution gradient of sodium chloride (right axis). NNC, non-negatively charged ^{35}S-labelled material eluting in the buffer wash.

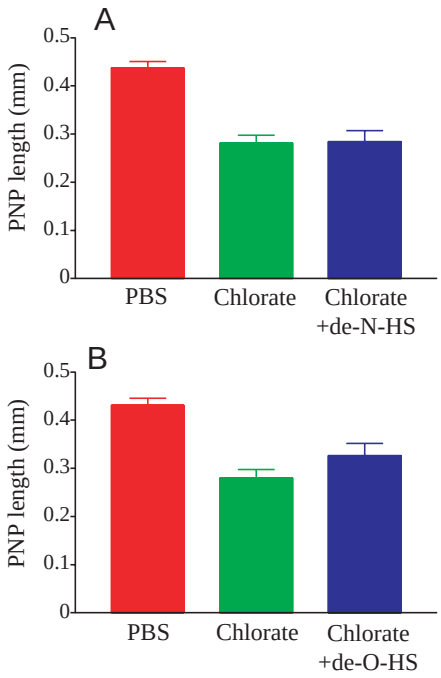

Fig. 5. Importance of N- and O-sulphate groups in heparan sulphate. Embryos were cultured in the presence of PBS, 30 mM chlorate alone or 30 mM chlorate plus (A) 100 ng/ml de-N-sulphated or (B) 100 ng/ml de-O-sulphated heparan sulphate. Posterior neuropore length varies significantly between treatment groups (one-way ANOVA; $P<0.0001$) in both panels. Although the chlorate-induced reduction in posterior neuropore length was statistically significant in both experiments (Dunnett's test; $P<0.01$ in both cases), there was no significant difference between embryos treated with chlorate alone and those treated additionally with de-N- or de-O-sulphated heparan sulphate ($P>0.05$). Values represent mean±s.e.m. of at least nine embryos per group. de-N-HS, de-N-sulphated heparan sulphate; de-O-HS, de-O-sulphated heparan sulphate.

hinge points appear straight and rigid (Shum and Copp, 1996; Ybot-Gonzalez and Copp, 1999) (Ybot-Gonzalez et al., 2002). Strikingly, embryos cultured in the presence of 30 mM chlorate do not have a median hinge point (Fig. 6F). Instead, the midline neural plate is flat, or even convex, whereas bending at the paired dorsolateral hinge points is accentuated, and this appears to compensate for the lack of a median hinge point in bringing the neural fold apices towards the dorsal midline. The region of the neural plate between the paired dorsolateral hinge points appears to have lost its rigidity and buckles, yielding the convex appearance observed in whole embryos (Fig. 6B). Despite this abnormal neural plate morphology, immunohistochemical staining for activated caspase 3 does not provide evidence for increased programmed cell death in chlorate-treated embryos (not shown).

Formation of the chlorate-induced neuroepithelial morphology could be blocked by addition of exogenous sulphate to the culture medium (Fig. 6G), yielding a posterior neuropore morphology similar to that seen in embryos exposed only to PBS. This result correlates with the finding that exogenous sulphate blocks chlorate-induced premature posterior neuropore closure, and is consistent with competitive inhibition of GAG sulphation by chlorate.

Supplementation of the culture medium with exogenous heparan sulphate also prevents chlorate-induced changes in posterior neuropore morphology (Fig. 6C,H). This suggests that the exogenous heparan sulphate in the culture medium is an effective substitute for 'normally sulphated' heparan sulphate synthesised endogenously by the embryo, and correlates with the finding that exogenous heparan sulphate blocks chlorate-induced premature posterior neuropore

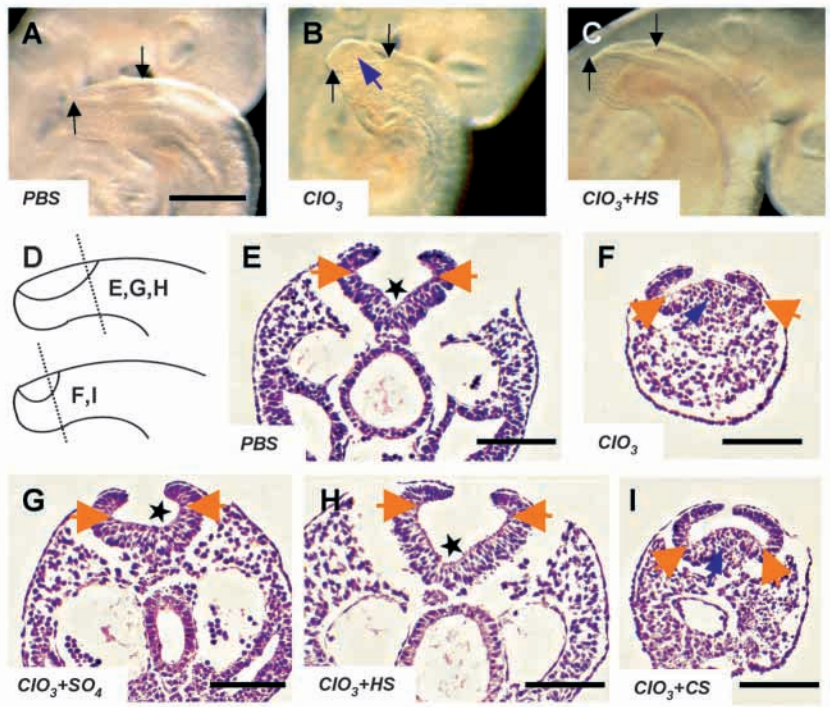

Fig. 6. Heparan sulphate affects neural plate bending during spinal neurulation. (A-C) E9.5 embryos following culture showing the normal appearance of the posterior neuropore (between black arrows) in embryos treated with PBS (A) and chlorate plus heparan sulphate (C). By contrast, embryos treated with chlorate alone exhibit a convex neural plate within a shortened neuropore (blue arrow in B). (E-I) H&E-stained transverse sections through the rostral end of the posterior neuropore of embryos cultured in the presence of PBS (E), chlorate (F), chlorate plus sulphate (G), chlorate plus heparan sulphate (H) or chlorate plus chondroitin-6-sulphate (I). Note the loss of median hinge point, accentuation of dorsolateral bending and convex neural plate (blue arrows) in F,I compared with the normal appearance in E,G,H. Level of sections is shown in D. Posterior neuropore is shorter in embryos in F,I, compared with those in E,G,H, so sections at the level of the rostral end of the neuropore are more distal: hence, the reduced section diameter in F,I. Reagent concentrations as in Fig. 3. Red arrows, paired dorsolateral hinge points; star, median hinge point; ClO_3, chlorate; CS, chondroitin sulphate; HS, heparan sulphate; SO_4, sulphate. Scale bars: 0.5 mm in A-C; 100 μm in E-I.

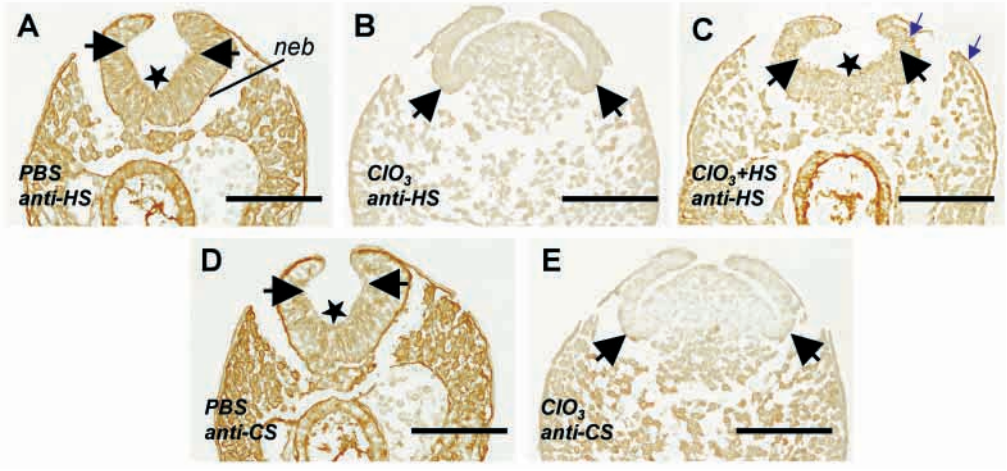

Fig. 7. Chlorate reduces the sulphation of GAGs in the posterior neuropore region. Immunohistochemical localisation of heparan sulphate (A-C) and chondroitin sulphate (D,E) on transverse sections through the posterior neuropore region prepared from embryos cultured in the presence of PBS (A,D), chlorate alone (B,E) or chlorate plus heparan sulphate (C). Heparan sulphate staining is reduced dramatically after chlorate treatment (B), whereas chlorate plus heparan sulphate-treated embryos show increased heparan sulphate staining, particularly in the ectodermal basement membrane (C, blue arrows), indicating access of exogenous heparan sulphate to embryonic tissues. Chondroitin sulphate exhibits specific loss of staining in the chlorate-treated neuroepithelium (E), whereas mesodermal staining is maintained at low intensity. Black arrows, paired dorsolateral hinge points; star, median hinge point; ClO_3, chlorate; CS, chondroitin sulphate; HS, heparan sulphate; neb, neuroepithelial basement membrane. Scale bars: 100 μm.

closure. By contrast, addition of exogenous chondroitin-6-sulphate to the culture medium does not prevent the chlorate-induced change in neuroepithelial morphology (Fig. 6I). In these embryos, the median hinge point is absent, the paired dorsolateral hinge points exhibit accentuated bending and neuroepithelial rigidity is lost in the region between the dorsolateral hinge points, as in embryos exposed to chlorate alone (Fig. 6F).

Chlorate diminishes immunostained GAGs in the mouse embryo

We assessed the presence of sulphated GAGs after chlorate treatment by immunostaining transverse sections of the posterior neuropore region with anti-heparan sulphate (10E4) and anti-chondroitin sulphate (CS-56) antibodies. Embryos cultured in the presence of PBS show strong staining for both heparan sulphate (Fig. 7A) and chondroitin sulphate (Fig. 7D) in the neuroepithelial basement membrane, extending from the median hinge point to the neural fold apices. Staining is also seen in the basement membrane of the surface ectoderm and gut endoderm, and in the extracellular matrix of the paraxial mesoderm. By contrast, staining for both sulphated GAGs is greatly reduced in chlorate-treated embryos. Staining for heparan sulphate is very weak throughout the section (Fig. 7B), whereas staining for chondroitin sulphate, although very much reduced in the neuroepithelium and neuroepithelial basement membrane, shows a less marked reduction than heparan sulphate in the underlying mesoderm (Fig. 7E). Importantly, chlorate-treated embryos exposed to exogenous heparan sulphate (Fig. 7C) exhibit an intensity of heparan sulphate staining that is intermediate between PBS-treated (Fig. 7A) and chlorate-treated embryos (Fig. 7B), with strongest staining in the surface ectodermal basement membrane and in the neural folds. This finding demonstrates that exogenous heparan sulphate, which is able to block the effect of chlorate on posterior neuropore closure, gains access to the cells of the posterior neuropore.

The persistent staining of chondroitin sulphate in chlorate-treated embryos contrasts with our finding of virtually no ^{35}S-labelled chondroitin sulphate detectable by ion-exchange chromatography after chlorate treatment (Fig. 4A). It seems likely that the anti-chondroitin sulphate antibody is detecting 'normally sulphated' chondroitin sulphate synthesised prior to the addition of chlorate to the culture medium, which must exhibit slower turnover than heparan sulphate. The overall reduction of 10E4 and CS-56 staining in the sections of chlorate-treated embryos suggests that sulphate groups comprise an important component of the epitopes recognised by these antibodies.

Effect of chlorate on sonic hedgehog signalling

Shh has been suggested to participate in the regulation of spinal neurulation by contributing to the formation of the median hinge point, while inhibiting bending at paired dorsolateral hinge points (Ybot-Gonzalez et al., 2002). To determine whether absence of the median hinge point and the accentuated bending at dorsolateral hinge points in chlorate-treated embryos may be related to disruption of Shh signalling, we compared the expression patterns of *Shh* and *Ptch* by in situ hybridisation. Shh is a ligand of Ptch and Shh signalling up-regulates *Ptch* expression (Goodrich et al., 1996; Marigo et al., 1996). Hence, an abnormal pattern of *Ptch* expression may indicate disruption of Shh signalling.

The expression patterns of *Shh* and *Ptch* transcripts in embryos cultured in the presence of PBS are essentially as described (Echelard et al., 1993; Goodrich et al., 1996). In the posterior neuropore region, *Shh* transcripts are detected in the notochord and in the ventral part of the hindgut (Fig. 8A), while *Ptch* transcripts are present in the neuroepithelium, particularly at the median hinge point, with staining intensity decreasing progressively towards the paired dorsolateral hinge points (Fig. 8C). The notochord is only weakly positive for *Ptch*, which is also seen in the hindgut (both dorsal and ventral parts) and weakly in mesoderm immediately lateral to gut and notochord.

Embryos cultured in the presence of chlorate exhibit a *Shh* expression pattern closely similar to that in PBS controls

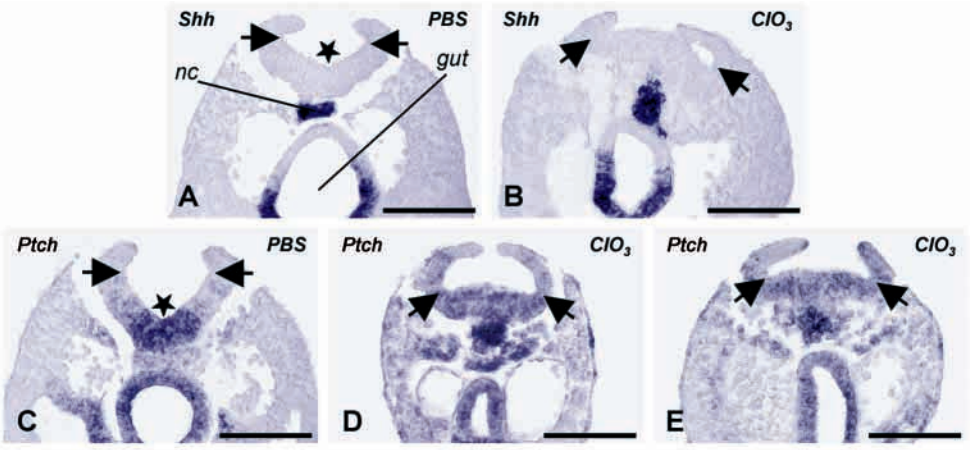

Fig. 8. Altered expression of *Ptch*, but not *Shh*, in embryos cultured in the presence of chlorate. Embryos cultured in the presence of either PBS (A,C) or 30 mM chlorate (B,D,E) were processed for whole-mount in situ hybridisation analysis of *Shh* (A,B) and *Ptch* (C-E), and then sectioned transversely through the rostral end of the posterior neuropore. The pattern of *Shh* expression does not differ between PBS-treated and chlorate-treated embryos (compare A with B), whereas the distribution of *Ptch* transcripts is markedly altered (compare C with D,E). In particular, notochordal expression of *Ptch* is strongly upregulated, as seen in two different chlorate-treated embryos (D,E), while midline neuroepithelial *Ptch* expression is less intense and exhibits less marked ventrodorsal variation. Arrows, paired dorsolateral hinge points; star, median hinge point; ClO_3, chlorate; nc, notochord. Scale bars: 100 μm.

(compare Fig. 8A with 8B). By contrast, the distribution of *Ptch* transcripts differs in several respects in chlorate-treated embryos (Fig. 8D,E). Notably, the notochord is more strongly positive for *Ptch* mRNA in chlorate treated embryos than PBS controls, whereas the overlying neuroepithelium exhibits weaker signal and the ventrodorsal gradient of expression is less pronounced. Furthermore, *Ptch* expression is less restricted to axial tissues: variable amounts of punctate staining are detected even in the most lateral paraxial mesoderm.

DISCUSSION

We have examined the role of heparan sulphate in spinal neurulation, using chlorate to competitively inhibit GAG sulphation. Chlorate specifically blocks median hinge point formation in the bending neural plate and accelerates closure of the posterior neuropore, the latter being mediated through accentuated bending at the paired dorsolateral hinge points. These chlorate-induced effects can be prevented by supplementation of the culture medium with 'normally sulphated' heparan sulphate, but not by addition of chondroitin sulphate, heparitinase-treated heparan sulphate or heparan sulphate lacking either the N- or O-linked sulphate groups. These findings are summarised in Table 1. Below, we consider the possible roles of HSPGs in neurulation through their influence on the actin cytoskeleton, the cell cycle and the propagation of molecular signals, including Shh.

Table 1. Summary of the effect of exogenous chlorate with or without other reagents on posterior neuropore length in cultured mouse embryos

Chlorate	Other reagent	Posterior neuropore length
–	–	Normal
+	–	↓
+	Carrier-free sulphate	Normal
+	Heparan sulphate	Normal
+	Heparitinase-treated heparan sulphate	↓
+	Chondroitin sulphate	↓
+	De-N-sulphated heparan sulphate	↓
+	De-O-sulphated heparan sulphate	↓

+, present; –, absent; ↓, decreased.

Differing actions of chlorate and β-D-xyloside

The accelerating effect of chlorate on spinal neurulation contrasts with the lack of effect of β-D-xyloside on posterior neuropore closure. The reason for this difference probably lies in the different biochemical actions of the two agents. Chlorate inhibits sulphation of GAG chains, but does not block their addition to the protein backbone, whereas β-D-xyloside acts as a substitute for xylose in the link between sulphated GAGs and their protein backbones, yielding 'naked' proteoglycan backbones and free, normally sulphated GAG chains. Our findings suggest that correct sulphation of heparan sulphate, but not its attachment to the protein backbone, is required for normal spinal neurulation, whereas intact proteoglycans appear to be necessary for cranial neurulation, which is inhibited by both β-D-xyloside and heparitinase (Morriss-Kay and Crutch, 1982; Tuckett and Morriss-Kay, 1989). Although the identity of the HSPGs that participate in neurulation is unclear, the presence of perlecan during mouse neurulation has been demonstrated (O'Shea, 1987; Trasler and Morriss-Kay, 1991).

Heparan sulphate and the role of actin microfilaments in neurulation

Actin microfilament bundles are found in neuroepithelial cells (Baker and Schroeder, 1967; Karfunkel, 1974; Morriss-Kay and Tuckett, 1985; Morriss and New, 1979; Nagele and Lee, 1980; Sadler et al., 1982; Ybot-Gonzalez and Copp, 1999) and their contraction has been postulated to cause neuroepithelial cell wedging, leading to elevation and bending of the neural folds (Karfunkel, 1974). Moreover, HSPGs are known to co-localise with, and bind to, actin and other components of the cytoskeleton in epithelial cells, thus participating in organisation of the cytoskeleton (Bernfield et al., 1999; Carey et al., 1994; Carey et al., 1996; Fernandez-Borja et al., 1995). Indeed, apical microfilament bundles in the cranial neuroepithelium were found to be poorly organised when cranial neural tube closure was inhibited by β-D-xyloside treatment of cultured rat embryos, which blocks the attachment of GAGs to their proteoglycan core proteins (Morriss-Kay and

Crutch, 1982). The breadth of the apical region of neuroepithelial cells was widened in these embryos, suggesting that the microfilament bundles were not under tension. Moreover, exposure of cultured mouse embryos undergoing spinal neurulation to cytochalasin D also resulted in disassembly of the apical microfilaments in the neuroepithelium (Ybot-Gonzalez and Copp, 1999). This led to loss of rigidity of the neural plate, resembling the morphology seen in chlorate-treated embryos. This suggests that microfilament assembly and contraction in the neuroepithelium require heparan sulphate, and that this heparan sulphate needs to be 'normally' sulphated. Importantly, however, formation of the median and dorsolateral hinge points during mouse spinal neurulation was not inhibited by cytochalasin D (Ybot-Gonzalez and Copp, 1999), indicating that additional factors must also act to prevent median hinge point formation in the chlorate-treated embryos.

Heparan sulphate and the cell cycle

Besides apical contraction, neuroepithelial cells may adopt a wedge shape by broadening of the cell base. This appears to be an important mechanism for hinge point formation during mouse spinal neurulation, in the absence of a requirement for actin microfilaments (Ybot-Gonzalez and Copp, 1999). Interkinetic nuclear migration results in the cell nucleus occupying a basal position during S- and early G_2-phases of the cell cycle, and this is accompanied by cell wedging. Indeed, more cells are in G_2-phase in the median hinge point than in non-bending regions of the neural plate of the chick embryo, and these cells have a prolonged cell cycle (Smith and Schoenwolf, 1987; Smith and Schoenwolf, 1988). Similarly, cells in the median hinge point have a higher S-phase labelling index but lower mitotic index than elsewhere in the spinal neuroepithelium of the mouse embryo (Gerrelli and Copp, 1997).

Nuclear heparan sulphate is known to influence the cell cycle (Fedarko et al., 1989; Fedarko and Conrad, 1986; Ishihara and Conrad, 1989). Heparan sulphate has been localised in the nuclei of hepatoma cells in culture, and these heparan sulphate molecules contain highly sulphated residues (Fedarko and Conrad, 1986). As the hepatoma cells become confluent and stop dividing, the amount of nuclear heparan sulphate increases up to threefold (Ishihara and Conrad, 1989). Heparan sulphate, extracted from confluent cell cultures and added to growing cells, is taken up and transported to the cell nuclei (Fedarko et al., 1989), leading to inhibition of cell division. By contrast, heparan sulphate obtained from cells in the logarithmic phase of growth is less effectively taken up and does not affect cell division. Thus, prolongation of the cell cycle in median hinge point cells during normal neurulation could require the presence of nuclear heparan sulphate. Accordingly, perturbation of sulphation of heparan sulphate by chlorate could cause cells in the median hinge point to progress through the cell cycle, resulting in loss of basal localisation of the cell nuclei and disruption of cell wedging.

Heparan sulphate on the cell surface and in the extracellular matrix is also able to regulate cell cycling through its interaction with growth factors (Conrad, 1998). Binding of FGF to high-affinity FGF receptors leads to dimerisation and mutual tyrosine phosphorylation of these receptors, resulting in biological effects such as cell proliferation (Schlessinger et al., 1995). The growth factor-receptor interaction is facilitated by heparan sulphate. However, heparan sulphate that inhibits FGF-stimulated cell proliferation has also been described. For example, inhibitory heparan sulphate prevents the human breast cancer cell line MDA-MB-231 from responding to FGF2 (Delehedde et al., 1996). MDA-MB-231 cells do not normally have a mitogenic response to FGF2, but blocking sulphation of heparan sulphate by chlorate enables these cells to respond to FGF2 and proliferate. Heparan sulphate that inhibits a mitogenic response to FGF1 and FGF7 has also been described (Bonneh-Barkay et al., 1997; Pye et al., 2000), and this inhibitory activity has been correlated with the sulphation pattern of heparan sulphate. Thus, cells in the median hinge point could have a prolonged cell cycle because of their inability to respond to growth factors (such as FGFs), owing to the inhibitory action of heparan sulphate. Blocking sulphation of heparan sulphate by chlorate treatment releases the cells from this inhibition, enabling their increased proliferation, and abolishing median hinge point formation.

Heparan sulphate and sonic hedgehog signalling

Heparan sulphate is required for localisation and propagation of the hedgehog signal (Bellaiche et al., 1998; Lin et al., 2000; The et al., 1999) through its interaction with the transmembrane protein Dispatched. This promotes the release of hedgehog from producing cells and helps to propagate the signal through the tissues to the receiving cells (Burke et al., 1999). In addition, a specific requirement for sulphate groups on heparan sulphate is indicated by the disruption of hedgehog signalling where sulphation of heparan sulphate is perturbed, as in the *Drosophila sulfateless* mutant (The et al., 1999). Thus, it could be postulated that the absence of a median hinge point and the increased bending at the paired dorsolateral hinge points in the chlorate-treated embryos are caused by disruption of Shh signalling. Indeed, dorsolateral bending of the neural plate in the posterior neuropore has been shown to be negatively regulated by Shh (Ybot-Gonzalez et al., 2002). However, induction of midline bending by the notochord (Smith and Schoenwolf, 1989; Van Straaten et al., 1985) does not appear to depend primarily on Shh action. For example, median hinge point formation is not abolished in embryos lacking Shh function (Ybot-Gonzalez et al., 2002). We conclude that modulation of Shh function may be responsible for some, but not all, of the abnormalities of posterior neuropore closure observed in chlorate-treated embryos.

We have shown that chlorate alters the expression pattern of *Ptch* mRNA, whereas *Shh* expression appears unaffected. We cannot exclude the possibility that *Ptch* expression is affected directly by chlorate, or indirectly affected by altered neural plate bending. Nevertheless, our results are consistent with a reduced propagation of the Shh signal in the presence of chlorate. It is well established that the influence of Shh from the notochord and floor plate induces a ventrodorsal gradient of *Ptch* expression in the neuroepithelium (Marigo and Tabin, 1996). We suggest that during normal development, Shh signalling from the notochord is propagated towards the overlying neuroepithelium through the action of heparan sulphate in the intervening extracellular matrix. This suggestion is supported by the immunohistochemical studies

of Martí et al. (Martí et al., 1995), which show that Shh peptide is 'cleared' from notochordal cells (despite continuing *Shh* transcription in these cells) and accumulates in the adjacent floor plate region of E9.5 mouse embryos [see Figure 5F,G by Martí et al. (Martí et al., 1995)]. We suggest, moreover, that inhibition of heparan sulphation by chlorate treatment abolishes this propagation of the Shh signal. Shh peptide is now able to induce strong expression of *Ptch* within the notochord, at the site of Shh production, as well as in adjacent paraxial mesodermal cells that normally receive only low concentrations of Shh peptide, whereas *Ptch* is induced to a lesser degree in the overlying neuroepithelium, and the dorsoventral gradient of neuroepithelial *Ptch* expression is diminished.

The situation we observe in chlorate-treated mouse embryos differs from that in the *Drosophila tout-velu* mutant, where Ptc protein is absent, rather than ectopically expressed (Bellaiche et al., 1998). This difference could be explained by a quantitative and qualitative difference in heparan sulphate. In the *tout-velu* mutant, heparan sulphate is almost undetectable, owing to a lack of heparan sulphate co-polymerase, which is required for chain elongation (Toyoda et al., 2000). By contrast, chlorate treatment merely inhibits O-sulphation and, to a lesser extent N-sulphation, and does not have a significant effect on chain elongation or other structural modifications of heparan sulphate (Conrad, 1998; Greve et al., 1988; Safaiyan et al., 1999).

In conclusion, we have demonstrated a role for HSPGs in regulating mouse spinal neurulation. This role seems likely to be mediated via a combination of the effects of heparan sulphate on the cytoskeleton, cell cycle and the propagation of extracellular signals.

We are grateful to Andrew McMahon and Matthew Scott for kind gifts of the *Shh* and *Ptch* plasmids. This work was supported by the Wellcome Trust (A. J. C.) and by an Overseas Graduate Scholarship from the National University of Singapore (G. W. Y.).

REFERENCES

Avnur, Z. and Geiger, B. (1984). Immunocytochemical localization of native chondroitin-sulfate in tissues and cultured cells using specific monoclonal antibody. *Cell* **38**, 811-822.

Baker, P. C. and Schroeder, T. E. (1967). Cytoplasmic filaments and morphogenetic movement in the amphibian neural tube. *Dev. Biol.* **15**, 432-450.

Bellaiche, Y., The, I. and Perrimon, N. (1998). *Tout-velu* is a *Drosophila* homologue of the putative tumour suppressor *EXT-1* and is needed for Hh diffusion. *Nature* **394**, 85-88.

Bernfield, M., Götte, M., Park, P. W., Reizes, O., Fitzgerald, M. L., Lincecum, J. and Zako, M. (1999). Functions of cell surface heparan sulfate proteoglycans. *Annu. Rev. Biochem.* **68**, 729-777.

Bonneh-Barkay, D., Shlissel, M., Berman, B., Shaoul, E., Admon, A., Vlodavsky, I., Carey, D. J., Asundi, V. K., Reich-Slotky, R. and Ron, D. (1997). Identification of glypican as a dual modulator of the biological activity of fibroblast growth factors. *J. Biol. Chem.* **272**, 12415-12421.

Brown, N. A. and Fabro, S. (1981). Quantitation of rat embryonic development *in vitro*: a morphological scoring system. *Teratology* **24**, 65-78.

Bullock, S. L., Fletcher, J. M., Beddington, R. S. P. and Wilson, V. A. (1998). Renal agenesis in mice homozygous for a gene trap mutation in the gene encoding heparan sulfate 2-sulfotransferase. *Genes Dev.* **12**, 1894-1906.

Burke, R., Nellen, D., Bellotto, M., Hafen, E., Senti, T. A., Dickson, B. J. and Basler, K. (1999). Dispatched, a novel sterol-sensing domain protein dedicated to the release of cholesterol-modified Hedgehog from signaling cells. *Cell* **99**, 803-815.

Carey, D. J., Bendt, K. M. and Stahl, R. C. (1996). The cytoplasmic domain of syndecan-1 is required for cytoskeleton association but not detergent insolubility. Identification of essential cytoplasmic domain residues. *J. Biol. Chem.* **271**, 15253-15260.

Carey, D. J., Stahl, R. C., Tucker, B., Bendt, K. A. and Cizmeci-Smith, G. (1994). Aggregation-induced association of syndecan-1 with microfilaments mediated by the cytoplasmic domain. *Exp. Cell Res.* **214**, 12-21.

Conrad, H. E. (1998). *Heparin-binding Proteins.* San Diego: Academic Press.

Copp, A. J. and Bernfield, M. (1988). Glycosaminoglycans vary in accumulation along the neuraxis during spinal neurulation in the mouse embryo. *Dev. Biol.* **130**, 573-582.

Copp, A. J. and Bernfield, M. (1994). Etiology and pathogenesis of human neural tube defects: Insights from mouse models. *Curr. Opin. Pediatr.* **6**, 624-631.

Copp, A. J., Brook, F. A., Estibeiro, P., Shum, A. S. W. and Cockroft, D. L. (1990). The embryonic development of mammalian neural tube defects. *Prog. Neurobiol.* **35**, 363-403.

Copp, A. J., Cogram, P., Fleming, A., Gerrelli, D., Henderson, D. J., Hynes, A., Kolatsi-Joannou, M., Murdoch, J. and Ybot-Gonzalez, P. (2000). Neurulation and neural tube closure defects. In *Developmental Biology Protocols, Vol. II* (ed. R. S. Tuan and C. W. Lo), pp. 135-160. Totowa: Humana Press.

David, G., Bai, X. M., Van-der, S. B., Cassiman, J. J. and Van-den, B. H. (1992). Developmental changes in heparan sulfate expression: *in situ* detection with mAbs. *J. Cell Biol.* **119**, 961-975.

Davies, J., Lyon, M., Gallagher, J. and Garrod, D. (1995). Sulphated proteoglycan is required for collecting duct growth and branching but not nephron formation during kidney development. *Development* **121**, 1507-1517.

Delehedde, M., Deudon, E., Boilly, B. and Hondermarck, H. (1996). Heparan sulfate proteoglycans play a dual role in regulating fibroblast growth factor-2 mitogenic activity in human breast cancer cells. *Exp. Cell Res.* **229**, 398-406.

Deng, C., Bedford, M., Li, C., Xu, X., Yang, X., Dunmore, J. and Leder, P. (1997). Fibroblast growth factor receptor-1 (FGFR-1) is essential for normal neural tube and limb development. *Dev. Biol.* **185**, 42-54.

Echelard, Y., Epstein, D. J., St-Jacques, B., Shen, L., Mohler, J., McMahon, J. A. and McMahon, A. P. (1993). Sonic hedgehog, a member of a family of putative signaling molecules, is implicated in the regulation of CNS polarity. *Cell* **75**, 1417-1430.

Fedarko, N. S. and Conrad, H. E. (1986). A unique heparan sulfate in the nuclei of hepatocytes: structural changes with the growth state of the cells. *J. Cell Biol.* **102**, 587-599.

Fedarko, N. S., Ishihara, M. and Conrad, H. E. (1989). Control of cell division in hepatoma cells by exogenous heparan sulfate proteoglycan. *J. Cell Physiol.* **139**, 287-294.

Fernandez-Borja, M., Bellido, D., Makiya, R., David, G., Olivecrona, G., Reina, M. and Vilaró, S. (1995). Actin cytoskeleton of fibroblasts organizes surface proteoglycans that bind basic fibroblast growth factor and lipoprotein lipase. *Cell Motil. Cytoskel.* **30**, 89-107.

Gerrelli, D. and Copp, A. J. (1997). Failure of neural tube closure in the *loop-tail* (*Lp*) mutant mouse: analysis of the embryonic mechanism. *Dev. Brain Res.* **102**, 217-224.

Gofflot, F., Hall, M. and Morriss-Kay, G. M. (1998). Genetic patterning of the posterior neuropore region of *curly tail* mouse embryos: deficiency of *Wnt5a* expression. *Int. J. Dev. Biol.* **42**, 637-644.

Goodrich, L. V., Johnson, R. L., Milenkovic, L., McMahon, J. A. and Scott, M. P. (1996). Conservation of the *hedgehog*/*patched* signaling pathway from flies to mice: induction of a mouse *patched* gene by Hedgehog. *Genes Dev.* **10**, 301-312.

Greve, H., Cully, Z., Blumberg, P. and Kresse, H. (1988). Influence of chlorate on proteoglycan biosynthesis by cultured human fibroblasts. *J. Biol. Chem.* **263**, 12886-12892.

Häcker, U., Lin, X. and Perrimon, N. (1997). The *Drosophila sugarless* gene modulates Wingless signaling and encodes an enzyme involved in polysaccharide biosynthesis. *Development* **124**, 3565-3573.

Ishihara, M. and Conrad, H. E. (1989). Correlations between heparan sulfate metabolism and hepatoma growth. *J. Cell Physiol.* **138**, 467-476.

Karfunkel, P. (1974). The mechanisms of neural tube formation. *Int. Rev. Cytol.* **38**, 245-271.

Lin, X., Buff, E. M., Perrimon, N. and Michelson, A. M. (1999). Heparan sulfate proteoglycans are essential for FGF receptor signaling during *Drosophila* embryonic development. *Development* **126**, 3715-3723.

Lin, X., Wei, G., Shi, Z., Dryer, L., Esko, J. D., Wells, D. E. and Matzuk, M. M. (2000). Disruption of gastrulation and heparan sulfate biosynthesis in EXT1-deficient mice. *Dev. Biol.* **224**, 299-311.

Marigo, V. and Tabin, C. J. (1996). Regulation of *Patched* by Sonic hedgehog in the developing neural tube. *Proc. Natl. Acad. Sci. USA* **93**, 9346-9351.

Marigo, V., Davey, R. A., Zuo, Y., Cunningham, J. M. and Tabin, C. J. (1996). Biochemical evidence that Patched is the Hedgehog receptor. *Nature* **384**, 176-179.

Martí, E., Takada, R., Bumcrot, D. A., Sasaki, H. and McMahon, A. P. (1995). Distribution of Sonic hedgehog peptides in the developing chick and mouse embryo. *Development* **121**, 2537-2547.

Miao, H.-Q., Ishai-Michaeli, R., Atzmon, R., Peretz, T. and Vlodavsky, I. (1996). Sulfate moieties in the subendothelial extracellular matrix are involved in basic fibroblast growth factor sequestration, dimerization, and stimulation of cell proliferation. *J. Biol. Chem.* **271**, 4879-4886.

Morriss-Kay, G. and Tuckett, F. (1985). The role of microfilaments in cranial neurulation in rat embryos: effects of short-term exposure to cytochalasin D. *J. Embryol. Exp. Morphol.* **88**, 333-348.

Morriss-Kay, G. M. and Crutch, B. (1982). Culture of rat embryos with β-D-xyloside: evidence of a role for proteoglycans in neurulation. *J. Anat.* **134**, 491-506.

Morriss, G. M. and New, D. A. T. (1979). Effect of oxygen concentration on morphogenesis of cranial neural folds and neural crest in cultured rat embryos. *J. Embryol. Exp. Morphol.* **54**, 17-35.

Nagele, R. G. and Lee, H. (1980). Studies on the mechanisms of neurulation in the chick: microfilament-mediated changes in cell shape during uplifting of neural folds. *J. Exp. Zool.* **213**, 391-398.

O'Shea, K. S. (1987). Differential deposition of basement membrane components during formation of the caudal neural tube in the mouse embryo. *Development* **99**, 509-519.

Pye, D. A., Vivès, R. R., Hyde, P. and Gallagher, J. T. (2000). Regulation of FGF-1 mitogenic activity by heparan sulfate oligosaccharides is dependent on specific structural features: differential requirements for the modulation of FGF-1 and FGF-2. *Glycobiology* **10**, 1183-1192.

Ringvall, M., Ledin, J., Holmborn, K., van Kuppevelt, T., Ellin, F., Eriksson, I., Olofsson, A., Kjellen, L. and Forsberg, E. (2000). Defective heparan sulfate biosynthesis and neonatal lethality in mice lacking N-deacetylase/N-sulfotransferase-1. *J. Biol. Chem.* **275**, 25926-25930.

Sadler, T. W., Greenberg, D., Coughlin, P. and Lessard, J. L. (1982). Actin distribution patterns in the mouse neural tube during neurulation. *Science* **215**, 172-174.

Safaiyan, F., Kolset, S. O., Prydz, K., Gottfridsson, E., Lindahl, U. and Salmivirta, M. (1999). Selective effects of sodium chlorate treatment on the sulfation of heparan sulfate. *J. Biol. Chem.* **274**, 36267-36273.

Schlessinger, J., Lax, I. and Lemmon, M. (1995). Regulation of growth factor activation by proteoglycans: what is the role of the low affinity receptors? *Cell* **83**, 357-360.

Shum, A. S. and Copp, A. J. (1996). Regional differences in morphogenesis of the neuroepithelium suggest multiple mechanisms of spinal neurulation in the mouse. *Anat. Embryol.* **194**, 65-73.

Smith, J. L. and Schoenwolf, G. C. (1987). Cell cycle and neuroepithelial cell shape during bending of the chick neural plate. *Anat. Rec.* **218**, 196-206.

Smith, J. L. and Schoenwolf, G. C. (1988). Role of cell-cycle in regulating neuroepithelial cell shape during bending of the chick neural plate. *Cell Tissue Res.* **252**, 491-500.

Smith, J. L. and Schoenwolf, G. C. (1989). Notochordal induction of cell wedging in the chick neural plate and its role in neural tube formation. *J. Exp. Zool.* **250**, 49-62.

Smith, J. L. and Schoenwolf, G. C. (1997). Neurulation: coming to closure. *Trends Neurosci.* **20**, 510-517.

Solursh, M. and Morriss, G. M. (1977). Glycosaminoglycan synthesis in rat embryos during the formation of the primary mesenchyme and neural folds. *Dev. Biol.* **57**, 75-86.

Tautz, D. and Pfeiffle, C. (1989). A nonradioactive *in situ* hybridization method for the localization of specific RNAs in *Drosophila* embryos reveals a translational control of the segmentation gene hunchback. *Chromosoma* **98**, 81-85.

The, I., Bellaiche, Y. and Perrimon, N. (1999). Hedgehog movement is regulated through *tout velu*-dependent synthesis of a heparan sulfate proteoglycan. *Mol. Cell* **4**, 633-639.

Toyoda, H., Kinoshita-Toyoda, A., Fox, B. and Selleck, S. B. (2000). Structural analysis of glycosaminoglycans in animals bearing mutations in *sugarless*, *sulfateless*, and *tout-velu*. *Drosophila* homologues of vertebrate genes encoding glycosaminoglycan biosynthetic enzymes. *J. Biol. Chem.* **275**, 21856-21861.

Trasler, D. G. and Morriss-Kay, G. (1991). Immunohistochemical localization of chondroitin and heparan sulfate proteoglycans in pre-spina bifida splotch mouse embryos. *Teratology* **44,** 571-579.

Tuckett, F. and Morriss-Kay, G. M. (1989). Heparitinase treatment of rat embryos during cranial neurulation. *Anat. Embryol.* **180**, 393-400.

Van Straaten, H. W. M., Thors, F., Wiertz-Hoessels, J., Hekking, J. and Drukker, J. (1985). Effect of a notochordal implant on the early morphogenesis of the neural tube and neuroblasts: Histometrical and histological results. *Dev. Biol.* **110**, 247-254.

Van Straaten, H. W. M., Hekking, J. W. M., Copp, A. J. and Bernfield, M. (1992). Deceleration and acceleration in the rate of posterior neuropore closure during neurulation in the curly tail (ct) mouse embryo. *Anat. Embryol.* **185**, 169-174.

Ybot-Gonzalez, P. and Copp, A. J. (1999). Bending of the neural plate during mouse spinal neurulation is independent of actin microfilaments. *Dev. Dyn.* **215**, 273-283.

Ybot-Gonzalez, P., Cogram, P., Gerrelli, D. and Copp, A. J. (2002). Sonic hedgehog and the molecular regulation of mouse neural tube closure. *Development* (in press).